Progress In Electromagnetics Research, Vol. 110, 219–235, 2010

ON THE CHARACTERISTIC IMPEDANCE DEFINITION IN MICROSTRIP AND COPLANAR LINES

W. Marynowski, P. Kowalczyk, and J. Mazur †

Faculty of Electronics, Telecommunications and Informatics (ETI)
Gdansk University of Technology (GUT), Gdansk 80-952, Poland

Abstract—In this paper the definition of characteristic impedance for lossless microstrip and coplanar lines has been considered. It has been shown that due to a significant value of the displacement current related to longitudinal component of the electric field, impedance definition becomes ambiguous. Such ambiguity can cause considerable errors in design procedure. This effect is especially noticeable in the coplanar lines, in opposite to microstrip ones. To confirm the validity of the applied algorithm (spectral domain approach) the propagation coefficients and characteristic impedances have been compared to values obtained from commercial software.

1. INTRODUCTION

Coplanar strips on a dielectric substrate have been analyzed and utilized since 1970's [1–7], and they are still popular [8, 9] because they are easily adaptable to shunt-element connections without any penetration of the dielectric substrate. Such structures are also very useful in designing broadband antennas feeding structures [10–13]. However, the coplanar lines with a finite ground plane have been considered only in a few papers, mostly utilizing the quasistatic approximation [14].

The same applies to the case of microstrip lines. They have been widely utilized in microwave and RF devices since 1970's and are still developed and applied in new types of structures (metamaterials [15, 16], microstrip antennas [17], splitters [18] and filters [19]).

Received 3 September 2010, Accepted 29 October 2010, Scheduled 20 November 2010
Corresponding author: Piotr Kowalczyk (pio.kow@gmail.com).
† Also with Telecommunication Research Institute
233A J. Hallera Str., Gdansk 80-502, Poland.

Nowadays, the analysis of coplanar and microstrip structures becomes crucial in the design of printed circuits. The increasing speed of digital electronic devices requires more complex analysis. For higher frequencies the circuit as well as the field parameters must be considered (circuit-field coupled problems). A standard printed circuit board should now be treated as a system of unshielded coplanar waveguides or even a radiating structure. Therefore, in order to analyze such devices full-wave analysis techniques must be used.

Despite the fact that commercial software performs the fullwave analysis, results are often related to circuit parameters. One of the most important parameters of the line is a characteristic impedance. In this paper characteristic impedance definition for coplanar and microstrip lines is considered. Due to the observed displacement current related to a longitudinal component of the electric field this definition becomes ambiguous for the considered lines.

The displacement currents has been widely discussed in the literature but only in the aspect related to transversal component of the electric field in lossy media [20]. The longitudinal one has always been neglected in the analysis of these lines.

In order to show the influence of the displacement current on characteristic impedance, the analysis is restricted to a lossless dielectric materials. In such a case the conducting currents (in metal strips) and longitudinal displacement currents (in substrate) are in phase. As a result, the characteristic impedance is purely real.

The displacement currents in the analyzed structures can reach high values and must be taken into account in the formulas defining characteristic impedance. This effect is especially noticeable for coplanar lines — in one of the exemplary structures the impedance varies from $69\,\Omega$ to $128\,\Omega$.

2. METHOD OF ANALYSIS

In Fig. 1 the cross sections of the investigated lines are shown. The problem is solved using spectral domain approach (SDA) with the following Fourier transform definition:

$$\tilde{f}(p) = \int_{\mathbb{R}} f(y) e^{-jpy} dy, \quad f(y) = \frac{1}{2\pi} \int_{\mathbb{R}} \tilde{f}(p) e^{jpy} dp, \tag{1}$$

where $\tilde{f}(p)$ is the image of the function $f(y)$. The electromagnetic field in the structure can be described by Maxwell's equations defined in the

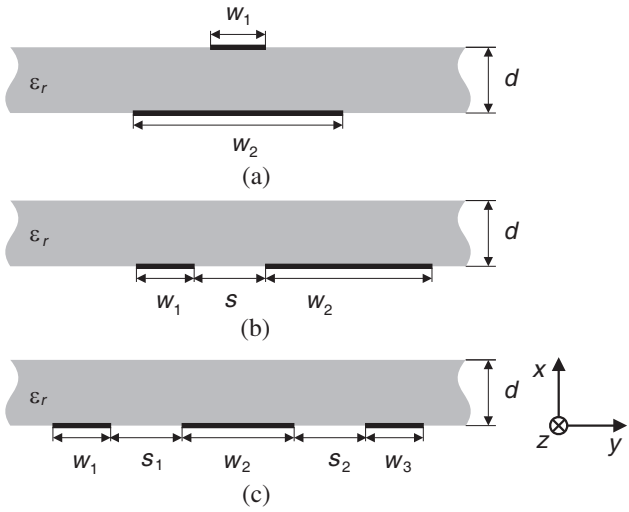

Figure 1. Cross sections of the analyzed structures. (a) Microstrip line with the reduced ground plane. (b) Coplanar two-strip line. (c) Coplanar three-strip line.

spectral domain, as follows:

$$\nabla \times \widetilde{\mathbf{E}}(x,p,z) = k_0 \eta \widetilde{\mathbf{H}}(x,p,z), \tag{2}$$

$$\nabla \times \eta \widetilde{\mathbf{H}}(x,p,z) = k_0 \varepsilon_r \widetilde{\mathbf{E}}(x,p,z), \tag{3}$$

where $\widetilde{\mathbf{E}}(x,p,z)$ and $\widetilde{\mathbf{H}}(x,p,z)$ are Fourier transforms of the electric and magnetic fields, respectively, $\eta = -j\sqrt{\mu_0/\varepsilon_0}$ and $k_0 = \omega\sqrt{\mu_0\varepsilon_0}$. By applying the boundary and continuity conditions to relations (2), (3) and assuming the fields and currents variation along z axis as $e^{-j\beta z}$, one obtains a set of equations combining tangential electric field ($\widetilde{E}_z$ and $\widetilde{E}_y$) and current densities ($\widetilde{J}_z$ and $\widetilde{J}_y$) at the strips:

$$\begin{bmatrix} \widetilde{E}_z(x=0,p) \\ \widetilde{E}_y(x=0,p) \end{bmatrix} = [\mathbf{G}(p,\beta)] \begin{bmatrix} \widetilde{J}_y(x=0,p) \\ \widetilde{J}_z(x=0,p) \end{bmatrix}, \tag{4}$$

where $\mathbf{G}(p,\beta)$ is a dyadic Green's function [6]. An application of Galerkin method to expression (4) with the standard basis

functions [21] expanding currents densities on the strips:

$$J_y(y) = \begin{cases} \sum\limits_{n=1}^{N} a_y \sin\left(\frac{n\pi(2y+w)}{2w}\right), & |y| \le \frac{w}{2} \\ 0, & \text{otherwise} \end{cases} \tag{5}$$

$$J_z(y) = \begin{cases} \sum\limits_{n=1}^{N} a_z \frac{\cos\left(\frac{(n-1)\pi(2y+w)}{2w}\right)}{\sqrt{1-\left(\frac{2y}{w}\right)^2}}, & |y| \le \frac{w}{2} \\ 0, & \text{otherwise,} \end{cases} \tag{6}$$

leads to a system of linear homogenous equations. The solution of this problem provides us with a normalized phase coefficient $\beta_n = \beta/k_0$, which allows us to determine the current density distribution on the strips as well as the electric and magnetic fields in the cross section of the structure.

The currents I on the strip can be calculated by an integration of the current densities $J_z(y)$ over the strip width

$$I = \int\limits_{-\frac{w}{2}}^{\frac{w}{2}} J_z(y)dy. \tag{7}$$

In order to avoid numerical integration errors, which are introduced in the evaluation of the singular basis functions, the following property of the Fourier transform is used [22]

$$\int\limits_{\mathbb{R}} f(y)dy = \tilde{f}(p=0). \tag{8}$$

As mentioned in the introduction, the longitudinal displacement current must be taken into account in the analysis of such structures. This current can be derived from Ampere's law applied to a whole cross section of the line (see Fig. 2):

$$\oint\limits_{L} \mathbf{H} \cdot \mathbf{dl} = \mathrm{j}\omega \iint\limits_{S} \mathbf{D} \cdot \mathbf{ds}, \tag{9}$$

where $L = L_1 \cup L_2 \cup L_3$ and $S = S_1 \cup S_2 \cup S_3$. Assuming that the fields far from the structure can be neglected, the following relation is

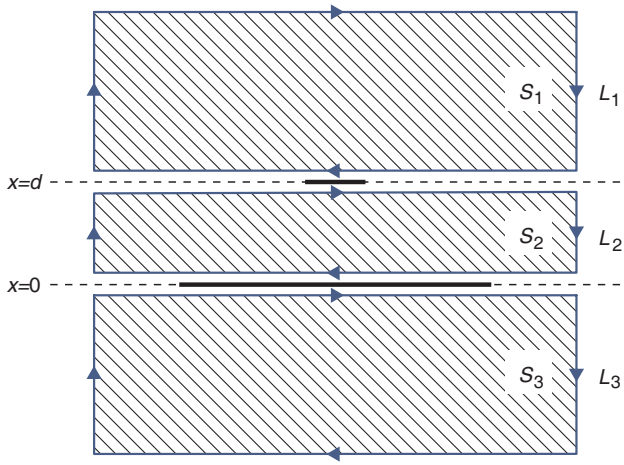

Figure 2. Cross section of the structure; L_1, L_2, L_3 — contours, S_1, S_2, S_3 — surfaces.

obtained [‡]:

$$\int_{\mathbb{R}} \left[H_y(d^+, y) - H_y(d^-, y)\right] dy + \int_{\mathbb{R}} \left[H_y(0^+, y) - H_y(0^-, y)\right] dy$$
$$= j\omega \iint_{\mathbb{R}^2} \varepsilon_r(x, y)\varepsilon_0 E_z(x, y) dxdy. \tag{10}$$

The magnetic field is discontinuous at the metallization only. Therefore

$$-\int_{\mathbb{R}} J_z(d, y)dy - \int_{\mathbb{R}} J_z(0, y)dy = j\omega \iint_{\mathbb{R}^2} \varepsilon_r(x, y)\varepsilon_0 E_z(x, y)dxdy \tag{11}$$

and finally

$$-\sum_{n=1}^{N} I_n = I_d, \tag{12}$$

where I_n is a current on the n-th strip, and N is the total number of the strips in the structure. If the displacement current is zero, the forward and backward conducting currents are equal. This situation is observed for TEM guides and particular types of the symmetrical quasi-TEM lines [3, 14].

[‡] For coplanar lines, when all strips are placed in the same plane (see Figs. 1(b) and (c)), the considerations can be reduced to the one plane only $x = 0$.

In general, for the quasi-TEM configuration, there are three different definitions of the characteristic impedance: voltage-current, voltage-power and power-current one. As far as the electric field in the analyzed structures is not potential ($curl(\mathbf{E}) \neq \mathbf{0}$), the voltage between two points depends on the path of the integration and might not be unique. However, the value of the current can be determined accurately (7). Therefore, to evaluate the characteristic impedance of the lines the current-power definition is chosen as:

$$Z = \frac{2P}{I^2}. \tag{13}$$

The power P is derived from Poynting vector on the cross section of the structure. In order to reduce the numerical errors in the fields evaluation the Parseval theorem is applied

$$P = \frac{1}{2}\Re\left[\iint\limits_{\mathbb{R}^2} S_z(x,y)dxdy\right] = \frac{1}{4\pi}\Re\left[\iint\limits_{\mathbb{R}^2} \widetilde{S}_z(x,p)dxdp\right], \tag{14}$$

where $S_z = (\mathbf{E}_t \times \mathbf{H}_t^*)_z = \left(E_x H_y^* - E_y H_x^*\right)$.

Despite the unique definition (13), the value of the characteristic impedance cannot be simply calculated, due to the differences in the currents on the strips. For example, in the case of two-strip line (microstrip or coplanar) and non-zero displacement current, the conducting currents flowing in the strips can be different ($|I_1| \neq |I_2|$). Denoting the currents ratio by

$$k = \frac{|I_1|}{|I_2|} \tag{15}$$

the ratio of the characteristic impedances Z_1 and Z_2, which are calculated from (13) for I_1 and I_2, can be expressed as follows

$$\frac{Z_2}{Z_1} = k^2. \tag{16}$$

As shown in the next section, the coefficient k can reach high value (about 1.5). As a result, the impedance Z_2 is 2.25 times greater than Z_1.

3. NUMERICAL RESULTS

The numerical tests of two- and three-strip structures are presented below. In case of these lines the quasi-TEM modes as well as the surface mode TM_0 can propagate without cutoff frequency. However, only quasi-TEM modes are involved in the presented analysis.

Extensive numerical tests have shown that the choice of 7 basis functions (for both longitudinal and transversal currents) ensures a proper convergence of the procedure. The trapezoidal integration step is equal $\Delta p = 0.025\,\mathrm{mm}^{-1}$, whereas $p \in \langle -50, 50 \rangle\,\mathrm{mm}^{-1}$.

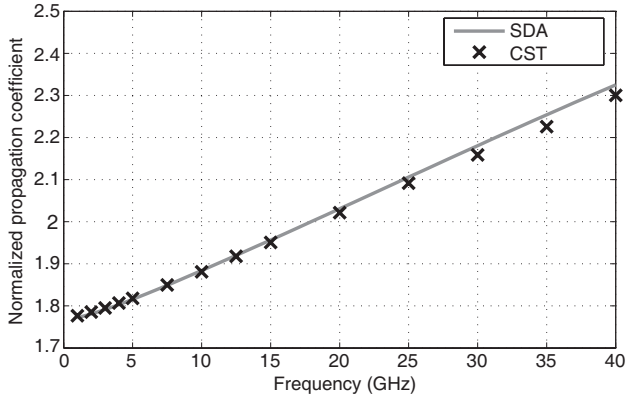

Figure 3. Propagation coefficient for the fundamental mode of the asymmetric structure (see Fig. 1(b)): $w_1 = 1\,\mathrm{mm}, s_1 = 1\,\mathrm{mm}$ and $w_2 = 8\,\mathrm{mm}$, $d = 0.635\,\mathrm{mm}$, $\varepsilon_r = 9.79$.

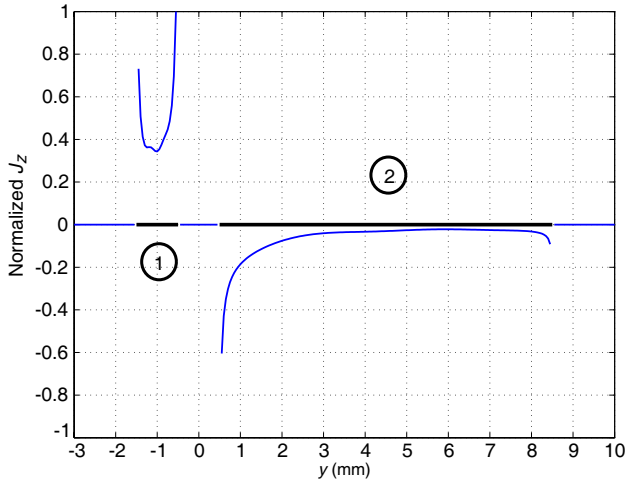

Figure 4. Current density distribution for the fundamental mode of the asymmetric structure (see Fig. 1(b)): $w_1 = 1\,\mathrm{mm}$, $s_1 = 1\,\mathrm{mm}$, $w_2 = 2\,\mathrm{mm}$, $d = 0.635\,\mathrm{mm}$, $\varepsilon_r = 9.79$.

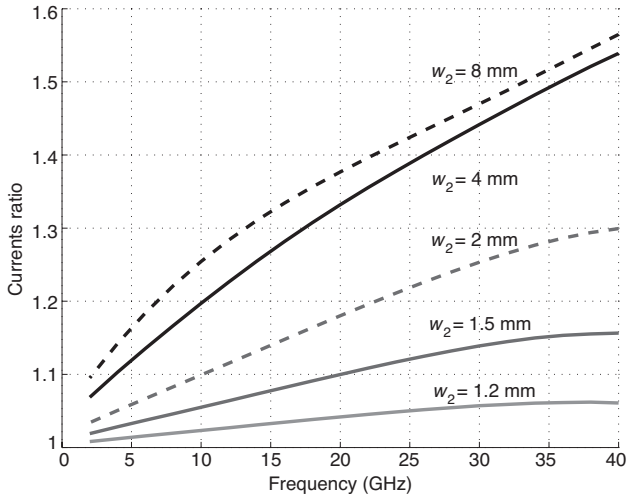

Figure 5. Currents ratio $k = |I_1/I_2|$ obtained in the analysis for the fundamental mode of the asymmetric structure (see Fig. 1(b)): $w_1 = 1\,\text{mm},\ s_1 = 1\,\text{mm},\ d = 0.635\,\text{mm},\ \varepsilon_r = 9.79$.

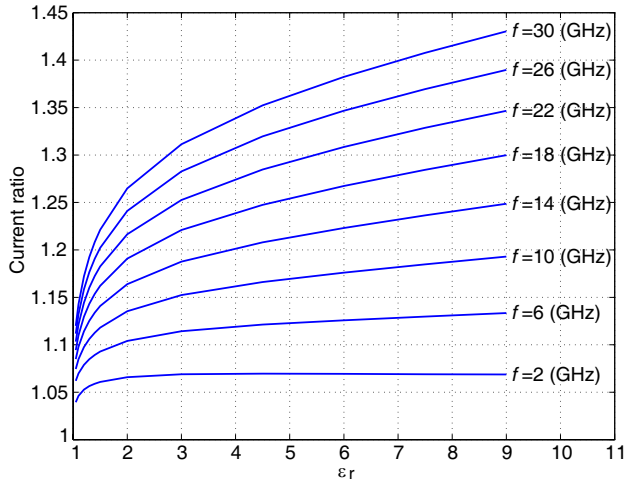

Figure 6. Currents ratio $k = |I_1/I_2|$ obtained in the analysis for the fundamental mode of the asymmetric structure (see Fig. 1(b)): $w_1 = 1\,\text{mm},\ s = 1\,\text{mm},\ w_2 = 4\,\text{mm},\ d = 0.635\,\text{mm}$.

3.1. Two-strip Structure

Firstly, a coplanar line composed of two strips of different widths is analyzed. In Fig. 3 a propagation coefficient for this asymmetric

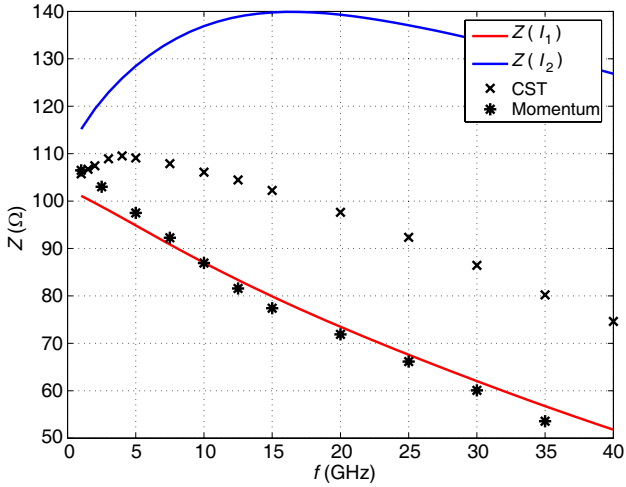

Figure 7. Characteristic impedance for the fundamental mode of the asymmetric structure (see Fig. 1(b)): $w_1 = 1\,\text{mm}$, $s_1 = 1\,\text{mm}$, $w_2 = 8\,\text{mm}$, $d = 0.635\,\text{mm}$, $\varepsilon_r = 9.79$.

configuration is presented and compared with the results of CST [23] simulations. A good agreement between the results obtained by both methods is achieved.

A current density distribution for the fundamental mode in that structure is shown in Fig. 4. Evaluation of currents in the strips (I_1 and I_2) exhibits a difference in their absolute values for higher frequencies, especially for high asymmetry of the structure. In Fig. 5 the ratio of the currents for a different asymmetry is presented. Moreover, for higher asymmetry the value of the coefficient k exceeds 1.5 for frequency close to 35 GHz. It must be emphasized that this effect is noticeable even for low values of the substrate permittivity (see Fig. 6).

The difference in the currents I_1 and I_2 results in the difference in the characteristic impedances. In Fig. 7 two impedance characteristics calculated for the currents I_1 and I_2 are presented. The results are compared with the ones obtained from commercial software (CST and ADS Momentum [24]).[§]

In Fig. 8 impedance characteristics obtained for different widths of the second strip in the coplanar line are collected. For high asymmetry (w_1=0.5 mm and w_2=8 mm) the impedance calculated for the first strip is 69 Ω whereas for the second strip 128 Ω. Similar analysis is performed

[§] It should be mentioned that for higher frequencies CST software generates warning about inaccuracies in the computation related with displacement current.

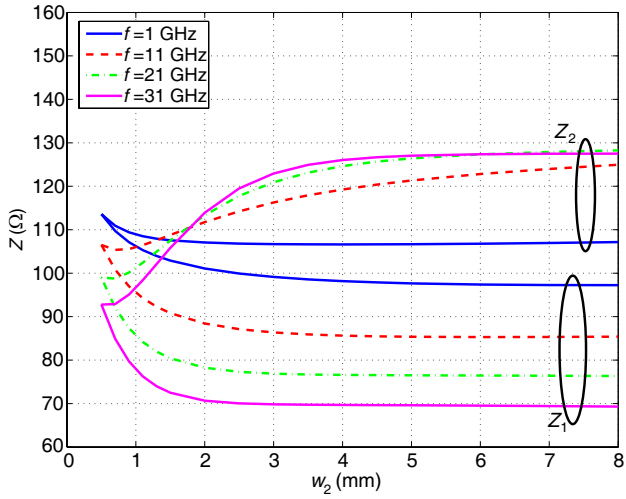

Figure 8. Characteristic impedance for the fundamental mode of the asymmetric coplanar structure (see Fig. 1(b)): $w_1 = 1\,\text{mm}$, $s_1 = 1\,\text{mm}$, $w_2 = 8\,\text{mm}$, $d = 0.635\,\text{mm}$, $\varepsilon_r = 9.79\,\text{mm}$.

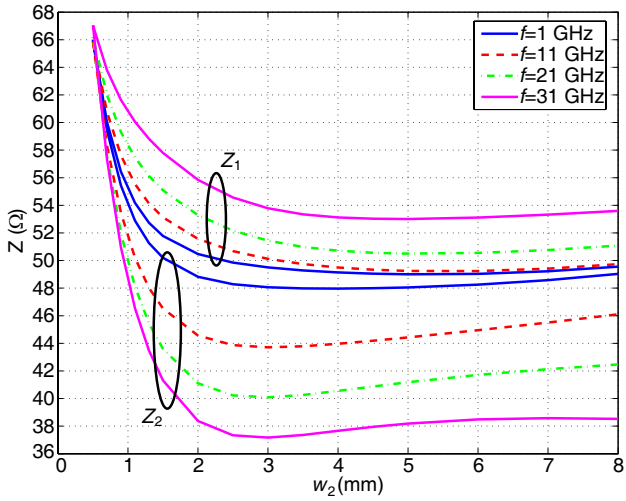

Figure 9. Characteristic impedance for the fundamental mode of the microstrip structure (see Fig. 1(a)): $w_1 = 1\,\text{mm}$, $w_2 = 8\,\text{mm}$, $d = 0.635\,\text{mm}$, $\varepsilon_r = 9.79$.

for the microstrip line (see Fig. 1(a)). In this case the impedance evaluated for a signal strip is more stable and changes from $49\,\Omega$ to

54 Ω, as shown in Fig. 9.

Generally, the displacement current in all analyzed structures is negligible for low frequencies, and the values of the currents I_1 and I_2 are equal. As a result, the impedances obtained from SDA, CST and ADS are the same.

In order to verify the validity of the algorithm the difference between the currents on the strips in the asymmetric structure and the evaluated displacement current are compared (see relation (12)). The displacement current is evaluated from the z component of the electric field (right-hand side of Equation (11)). The results for three different ranges of the integration are collected in Table 1. When the range is large enough, the displacement current I_d fulfills relation (12).

3.2. Three-strip Structure

In three-strip lines there are two fundamental (even and odd) modes. The first set of structure tests are preformed for even mode and low frequency and compared with the results obtained from quasistatic

Table 1. Currents in the asymmetric structure (see Fig. 1(b)): $w_1 = 1\,\text{mm}$, $s_1 = 1\,\text{mm}$, $w_2 = 4\,\text{mm}$, $d = 0.635\,\text{mm}$, $\varepsilon_r = 9.79$. Displacement current I_d is evaluated for different regions $\{(x, y) : |x| < x_n,\ |y| < y_n\}$, an origin of the coordinate system is located at the center of the slot.

Frequency (GHz)	$I_d\,(\mu\text{A})$			$(I_1 + I_2)\,(\mu\text{A})$
10	0.32887	0.38178	0.40424	−0.42390
20	0.61486	0.63458	0.63777	−0.64012
30	0.78177	0.78665	0.78693	−0.78921
$(x_n,\ y_n)$ (mm)	(4,8)	(6,12)	(8,16)	–

Table 2. Propagation coefficients and characteristic impedances of symmetric structure (see Fig. 1(c)): $f = 0.4\,\text{GHz}$, $w_1 = w_3 = w$, $s_1 = s_2 = s$, $w_2 = 1\,\text{mm}$, $d = 0.75\,\text{mm}$, $\varepsilon_r = 12.9$.

w (mm)	s (mm)	Normalized propagation coefficient		Characteristic impedance (Ω)		
		SDA	CST	From [14]	SDA	CST
2.5	2	2.099	2.089	72	87.8	82.7
1	0.5	2.470	2.443	49	49.9	48.3
0.625	0.125	2.583	2.504	34	29.9	27.2

approximation [14]. The results are collected in Table 2 (the values of the propagation coefficient evaluated in [14] are not presented here, due to the unclear description of the chart in [14]). It can be seen that the results obtained from all the methods are in a good agreement.

The frequency characteristics of the propagation coefficients of even and odd modes are depicted in Fig. 10. As one can see, these results agree well with the ones obtained from CST software. As far as the odd mode (with electric wall in the symmetry plane) is considered, the currents related with strips 1 and 3 have the opposite signs (see Fig. 11), whereas the total current on the strip 2 is equal

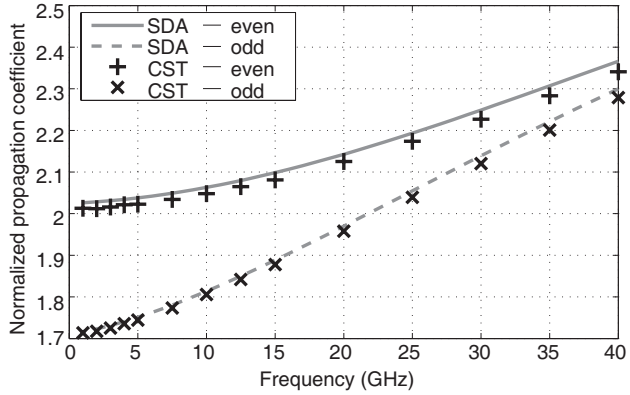

Figure 10. Propagation coefficient of the three strips line (see Fig. 1(c)): $w_1 = w_2 = w_3 = 1\,\text{mm}$, $s_1 = s_2 = 1\,\text{mm}$, $d = 0.635\,\text{mm}$, $\varepsilon_r = 9.79$.

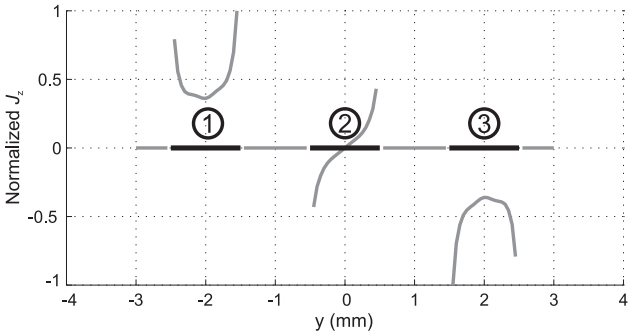

Figure 11. Currents density distributions of odd mode of the three strips structure (see Fig. 1(c)): $w_1 = w_2 = w_3 = 1\,\text{mm}$, $s_1 = s_2 = 1\,\text{mm}$, $d = 0.635\,\text{mm}$, $\varepsilon_r = 9.79$.

to 0. Therefore, $I_1 + I_2 + I_3 = 0$ and the displacement current I_d is zero because of antisymmetry of $E_z(x, y)$. In such a case the current I in (13) is unique, hence, the characteristic impedance $Z_{oddI_1} = Z_{oddI_3}$. The impedance of this structure is also evaluated using CST software, and a good agreement is achieved (see Fig. 12).

For even mode, when the magnetic wall is placed at a symmetry plane (see Fig. 13), the sum of all currents on the strips is not equal

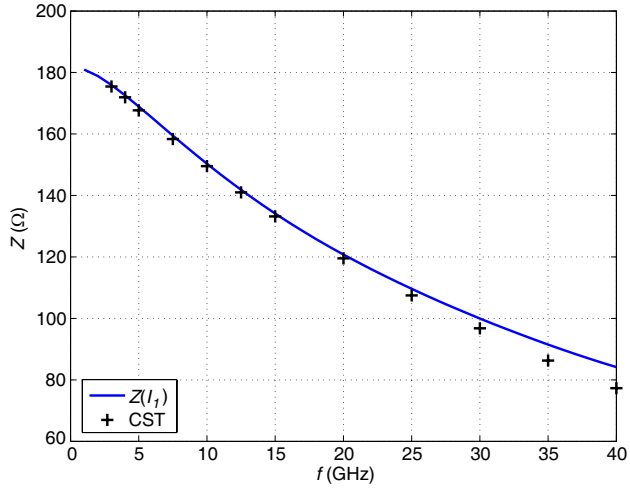

Figure 12. Characteristic impedance of the odd mode of the three strips line (see Fig. 1(c)): $w_1 = w_2 = w_3 = 1\,\text{mm}$, $s_1 = s_2 = 1\,\text{mm}$, $d = 0.635\,\text{mm}$, $\varepsilon_r = 9.79$.

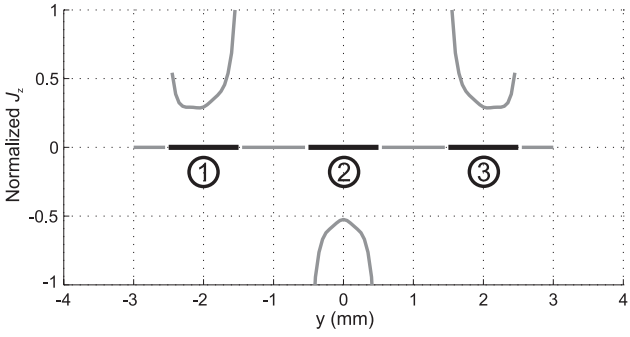

Figure 13. Currents density distributions of even mode of the three strips structure (see Fig. 1(c)): $w_1 = w_2 = w_3 = 1\,\text{mm}$, $s_1 = s_2 = 1\,\text{mm}$, $d = 0.635\,\text{mm}$, $\varepsilon_r = 9.79$.

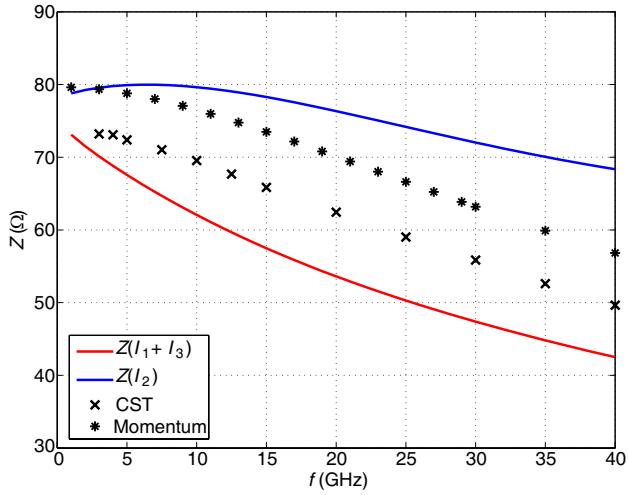

Figure 14. Characteristic impedance of the even mode of the three strips line (see Fig. 1(c)): $w_1 = w_2 = w_3 = 1\,\text{mm}$, $s_1 = s_2 = 1\,\text{mm}$, $d = 0.635\,\text{mm}$, $\varepsilon_r = 9.79$.

to zero. Due to the symmetry of $E_z(x, y)$, only if the displacement current I_d is taken into account the current equivalence relation (12) ($I_1 + I_2 + I_3 = -I_d$) is fulfilled. Similarly to the asymmetric two-strip line, two impedances involving different currents are evaluated: $Z_{even(I_1+I_3)}$ and $Z_{even(I_2)}$. The results obtained in the simulations are compared with the ones from CST and ADS Momentum (see Fig. 14). Also in this case the significant discrepancies in the characteristic impedances can be observed.

4. CONCLUSION

Microstrip and coplanar lossless lines have been investigated utilizing spectral domain approach. The results have been verified using commercial software CST and ADS Momentum. Special attention has been paid to the calculation of the displacement currents related to the longitudinal component of the electric field. It has been confirmed that the equivalence of the forward and backward currents in the structure can be achieved only if the displacement current is taken into account. It has been shown that the difference between the forward and backward conducting currents can be significant for the presented structures. As a result, the characteristic impedance cannot be uniquely defined. Finally, it has been shown that this

effect is especially noticeable in the coplanar structures even for low permittivity of the substrate.

ACKNOWLEDGMENT

The authors would like to thank Dr. V. Sokol from the Computer Simulation Technology for providing a 30-day trial version of Microwave Studio which was used in the presented work.

This work was supported by the Polish Ministry of Science and Higher Education in part from sources for science in the years 2007–2010 under Commissioned Research Project PBZ-MNiSW-DBO-04/I/2007 and in part from sources for science in the years 2010–2012 under COST Action IC0803, decision No. 618/N-COST/09/2010/0.

REFERENCES

1. Wen, C. P., "Coplanar-waveguide directional couplers," *IEEE Transactions on Microwave Theory and Techniques*, Vol. 18, No. 6, 318–322, June 1970.
2. Davis, M. E., E. W. Williams, and A. C. Celestini, "Finite-boundary corrections to the coplanar waveguide analysis," *IEEE Transactions on Microwave Theory and Techniques*, Vol. 21, No. 9, 594–596, September 1973.
3. Knorr, J. B. and K. Kuchler, "Analysis of coupled slots and coplanar strips on dielectric substrate," *IEEE Transactions on Microwave Theory and Techniques*, Vol. 23, No. 7, 541–548, July 1975.
4. Jansen, R. H., "Unified user-oriented computation of shielded, covered and open planar microwave and millimeter-wave transmission-line characteristics," *IEE Journal on Microwaves, Optics and Acoustics*, Vol. 3, No. 1, 14–22, January 1979.
5. Bhattacharya, D., "Characteristic impedance of coplanar waveguide," *Electronics Letters*, Vol. 21, No. 13, 557, June 1985.
6. Itoh, T., *Numerical Techniques for Microwave and Millimeter-Wave Passive Structures*, John Wiley & Sons, Inc., New York, 1989.
7. Mirshekar-Syahkal, D., *Spectral Domain Method for Microwave Integrated Circuits*, John Wiley & Sons, Inc., New York, 1990.
8. Stefanski, T. and B. J. Janiczak, "Analysis of single-ground-plane coplanar waveguide," *IEEE Microwave and Wireless Components Letters*, Vol. 16, No. 7, 395–397, July 2006.

9. Yildiz, C., K. Guney, M. Turkmen, and S. Kaya, "Neural models for coplanar strip line synthesis," *Progress In Electromagnetics Research*, Vol. 69, 127–144, 2007.
10. Si, L.-M. and X. Lv, "CPW-FED multi-band omni-directional planar microstrip antenna using composite metamaterial resonators for wireless communications," *Progress In Electromagnetics Research*, Vol. 83, 133–146, 2008.
11. Kumar, A. V. P., V. Hamsakutty, J. Yohannan, and K. T. Mathew, "Microstripline FED cylindrical dielectric resonator antenna with a coplanar parasitic strip," *Progress In Electromagnetics Research*, Vol. 60, 143–152, 2006.
12. Kanj, H. and M. Popovic, "A novel ultra-compact broadband antenna for microwave breast tumor detection," *Progress In Electromagnetics Research*, Vol. 86, 169–198, 2008.
13. Marynowski, W. and J. Mazur, "Design of UWB coplanar antenna with reduced ground plane," *Journal of Electromagnetic Waves and Applications*, Vol. 23, 1707–1713, 2009.
14. Görür, A. and C. Karpuz, "Effect of finite ground-plane widths on quasistatic parameters of asymmetrical coplanar waveguides," *IEE Proceedings — Microwaves, Antennas and Propagation*, Vol. 147, No. 5, 343–347, October 2000.
15. Monti, G. and L. Tarricone, "Negative group velocity in a split ring resonator-coupled microstrip line," *Progress In Electromagnetics Research*, Vol. 94, 33–47, 2009.
16. Abdelaziz, A. F., T. M. Abuelfadl, and O. L. Elsayed, "Realization of composite right/left-handed transmission line using coupled lines," *Progress In Electromagnetics Research*, Vol. 92, 299–315, 2009.
17. Vazquez Antuna, C., G. Hotopan, S. Ver Hoeye, M. Fernandez Garcia, L. F. Herran Ontanon, and F. Las-Heras, "Microstrip antenna design based on stacked patches for reconfigurable two dimensional planar array topologies," *Progress In Electromagnetics Research*, Vol. 97, 95–104, 2009.
18. Aliakbarian, H., A. Enayati, G. A. E. Vandenbosch, and W. De Raedt, "Novel low-cost end-wall microstrip-to-waveguide splitter transition," *Progress In Electromagnetics Research*, Vol. 101, 75–96, 2010.
19. Wang, Z., Q. Lai, R.-M. Xu, B. Yan, W. Lin, and Y. Guo "A millimeter-wave ultra-wideband four-way switch filter module based on novel three-line microstrip structure band-pass filters," *Progress In Electromagnetics Research*, Vol. 94, 297–309, 2009.

20. Williams, D. F., B. K. Alpert, U. Arz, D. K. Walker, and H. Grabinski, "Causal characteristic impedance of planar transmission lines," *IEEE Transactions on Advanced Packaging*, Vol. 26, No. 2, 165–171, May 2003.
21. Schmidt, L. and T. Itoh, "Spectral domain analysis of dominant and higher order modes in fin-lines," *IEEE Transactions on Microwave Theory and Techniques*, Vol. 28, No. 9, 981–985, September 1980.
22. Knorr, J. B. and A. Tufekcioglu, "Spectral-domain calculation of microstrip characteristic impedance.," *IEEE Transactions on Microwave Theory and Techniques*, Vol. 23, No. 9, 725–728, September 1975.
23. CST microwave studio (CST MWS), https://www.cst.com.
24. Advanced design system — momentum, agilent technologies, http://www.agilent.com.